



ACADEMIC  
PRESS

Available online at [www.sciencedirect.com](http://www.sciencedirect.com)

SCIENCE @ DIRECT®

Journal of Sound and Vibration 261 (2003) 955–965

---

---

JOURNAL OF  
SOUND AND  
VIBRATION

---

---

[www.elsevier.com/locate/jsvi](http://www.elsevier.com/locate/jsvi)

Letter to the Editor

## Modelling a rotating shaft subjected to a high-speed moving force

C.C. Cheng\*, J.K. Lin

*Department of Mechanical Engineering, National Chung Cheng University, Chia-Yi 621, Taiwan, ROC*

Received 8 July 2002; accepted 23 September 2002

### 1. Introduction

Although the vibration characteristics of a rotating shaft has been investigated analytically, numerically, and experimentally [1–10], there are still some fundamental issues that remain open and need to be addressed. It is well known that modelling a rotating shaft based on Euler–Bernoulli beam theory is inadequate for flexural vibration analysis while the shaft is short and stubby due to neglecting the effects of rotary inertia and transverse shear deformation. Although Rayleigh beam model includes the rotary inertia effect, it can predict only a limited number of critical speeds [6]. Furthermore, as the Rayleigh beam coefficient and the rotational speed increase, the predictions of the natural frequency and the shaft deflection become unacceptable. The Timoshenko beam model has been typically used as the most comprehensive model in the derivation of equations of motion of a rotating shaft and many researchers have studied its characteristics in rotordynamics [6–10]. The equations of motion for a rotating shaft subject to moving loads based on Timoshenko theory can be derived using either Newton's method [7] or Hamilton's principle [10]. Then, the shaft deformation that is expressed in terms of either an inertial frame [7,10] or a co-ordinate system fixed to the rotating shaft [8] can be determined by using the modal analysis or the integral transformation method. However, this complicated model usually leads the natural frequency to be determined numerically when the rotating shaft is subject to a moving load.

The note is concerned with the dynamic response of a high-speed rotating, short shaft subjected to a high-speed moving load. Under this circumstance, the shear and rotary inertia effects must be captured for an accurate dynamic analysis. The present work focused on the aspect of the determination of the natural frequency analytically, so the Timoshenko beam model must be simplified in the modelling. Therefore, a modified-Rayleigh beam model is proposed to improve the prediction accuracy of the critical speed, the natural frequency and the shaft deformation of Rayleigh beam model. Compared with the Rayleigh beam model, the proposed beam model

---

\*Corresponding author.

*E-mail address:* [imeccc@ccu.edu.tw](mailto:imeccc@ccu.edu.tw) (C.C. Cheng).

simply includes the shear deformation that plays an important role for a short and stubby shaft in flexural vibration. Compared with the Timoshenko beam model, we make simplifications by neglecting the coupling effects induced from the shear deformation. However, several questions need to be answered in this note: (1) What are the advantages of this proposed model in calculating the vibration response and the natural frequency compared with the Timoshenko beam model? (2) Compared with the Timoshenko beam model, what are the differences in predicting the vibration response and the natural frequency? (3) What are the limitations of this proposed model? Motivated by these three questions, this paper formulates a rotating shaft through the Newton method, determines the natural frequencies and quantifies the differences in vibration responses between the Timoshenko beam and the proposed model in order to find the answers to the questions stated above.

### 2. Equation of motions for different beam models

Consider a moving load of amplitude  $P$  with a constant speed  $v$  acting on a uniform shaft of length  $\ell$  lying in the  $x$ – $z$  plane with both ends simply supported and rotating at a constant angular velocity  $\Omega$  as shown in Fig. 1. The shaft has cross-sectional area  $A$ , cross-sectional shape factor  $\kappa$ , Young’s modulus  $E$ , shear modulus  $G$  and density  $\rho$ . In the following the equation of motion based on Timoshenko beam theory was derived using Newtonian approach. Details of derivation of the equation of motion can be found in Ref. [6]

$$EI \frac{\partial^4 u(z, t)}{\partial z^4} - \left( \frac{\rho EI}{\kappa G} + \rho I \right) \frac{\partial^4 u(z, t)}{\partial z^2 \partial t^2} + j2\Omega \rho I \frac{\partial^3 u(z, t)}{\partial z^2 \partial t} + \rho A \frac{\partial^2 u(z, t)}{\partial t^2} - j2\Omega \frac{\rho^2 I}{\kappa G} \frac{\partial^3 u(z, t)}{\partial t^3} + \frac{\rho^2 I}{\kappa G} \frac{\partial^4 u(z, t)}{\partial t^4} = P\delta(z - vt) - \frac{EI}{\kappa AG} \frac{\partial^2}{\partial z^2} P\delta(z - vt) - j2\Omega \frac{\rho I}{\kappa AG} \frac{\partial}{\partial t} P\delta(z - vt) + \frac{\rho I}{\kappa AG} \frac{\partial^2}{\partial t^2} P\delta(z - vt), \tag{1}$$

where  $u(z, t)$  represents the transverse displacement of the rotating shaft and  $\delta(z - vt)$  is the Dirac delta function. Note that the coupling between flexural and torsional vibration due to mass

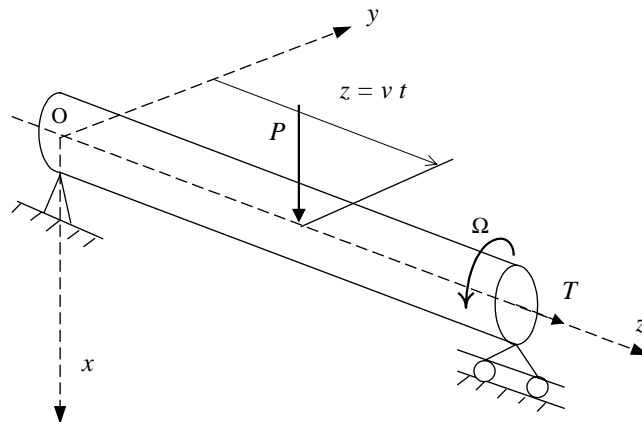


Fig. 1. Geometry of a spinning shaft subjected to a moving load.

eccentricity is not considered and the complex displacement  $u = u_x + ju_y$  is used for convenience in derivation [7]. The terms on the left-hand side in Eq. (1) include the flexural stiffness, the transverse shear and rotary inertia, the gyroscopic effect, the lateral inertia, the coupling between transverse shear and the gyroscopic effects and the coupling between transverse shear and the rotary inertia. In order to include the shear deformation which becomes significant when the cross-sectional dimensions are not small compared to the length of the beam in flexural vibration, a model based on Rayleigh beam theory, called the modified-Rayleigh beam model, is proposed. Compared with the Timoshenko beam model, the difference is that the shear angle is included in the modified-Rayleigh beam model in calculation of the bending moments and is reasonable only when the shear angle is small enough compared to the slope caused by the bending. However, the inclusion of the shear angle introduces the transverse shear, which proves to be important for a short and stubby shaft. Moreover, this approximation not only can simplify the equation of motion but also has the associate advantages described in the following sections. The equation of motion of the proposed modified-Rayleigh beam model is expressed as follows:

$$EI \frac{\partial^4 u(z, t)}{\partial z^4} - \left( \frac{\rho EI}{\kappa G} + \rho I \right) \frac{\partial^4 u(z, t)}{\partial z^2 \partial t^2} + j2\Omega \rho I \frac{\partial^3 u(z, t)}{\partial z^2 \partial t} + \rho A \frac{\partial^2 u(z, t)}{\partial t^2} = P\delta(z - vt) - \frac{EI}{\kappa AG} \frac{\partial^2}{\partial z^2} P\delta(z - vt). \quad (2)$$

Obviously, compared with the Rayleigh beam model, the modified-Rayleigh beam model simply takes into account the shear deformation effect. Nevertheless, compared with the Timoshenko beam model, this simplified model does not include the coupling effects induced by the shear deformation; such as the coupling between transverse shear and the gyroscopic effects and the coupling between transverse shear and the rotary inertia.

As stated in the introduction, the purpose of this study is to determine the advantages of this proposed model through determining the fundamental dynamic characteristics; such as the critical speed, the natural frequency and the deflection while the rotating shaft is subjected to a high-speed moving load. Moreover, we need to quantify the deviation in those characteristics between the Timoshenko beam model and the proposed model.

### 3. The displacement response and the natural frequency for a rotating shaft subjected to a moving load

The boundary and initial conditions for the system are expressed as  $u(0, t) = 0$ ,  $u(\ell, t) = 0$ ,  $\partial^2 u / \partial z^2(0, t) = 0$ ,  $\partial^2 u / \partial z^2(\ell, t) = 0$ ,  $u(z, 0) = 0$ ,  $\partial u / \partial t(z, 0) = 0$ ,  $\partial u / \partial z(z, 0) = 0$  and  $\partial^2 u / \partial t \partial z(z, 0) = 0$ . After applying the boundary and initial conditions, one can obtain the displacement responses in the  $x$  and  $y$  directions from the equations of motion of the respective beam models using the finite Fourier sine transformation and Laplace transform [7]. The displacement responses for the respective beam models are given as follows:

(a) *Modified-Rayleigh beam model:*

$$u_L(z, t) = (2/\ell) \sum_{n=1}^{\infty} \frac{d_L P \varpi_n}{a_L} (A_{L1} e^{j\omega_{Ln} t} + A_{L2} e^{j\omega_{Ln} t} + A_{L3} e^{j\varpi_n t} + A_{L4} e^{-j\varpi_n t}) \sin(n\pi z / \ell). \quad (3)$$

Here,  $A_{L1} \sim A_{L4}$  are listed in Appendix A  $d_L = 1 + EI/\kappa AG(n\pi/\ell)^2$ ,  $\varpi_n = n\pi v/\ell$  is the frequency caused by the moving load and the natural frequencies are

$$\omega_{Ln1,Ln2} = \frac{b_L\Omega \pm \sqrt{a_L c_L + b_L^2\Omega^2}}{a_L}, \tag{4}$$

where  $a_L = \rho A + (\rho EI/\kappa G + \rho I)(n\pi/\ell)^2$ ,  $b_L = \rho I(n\pi/\ell)^2$  and  $c_L = EI(n\pi/\ell)^4$ . Two natural frequencies,  $\omega_{Ln1}$  and  $\omega_{Ln2}$  correspond to the forward and the backward frequencies of the shaft, respectively. Both frequencies have an explicit form and can be determined analytically.

(b) *Timoshenko beam model:*

$$u_T(z, t) = (2/\ell) \sum_{n=1}^{\infty} \frac{P\varpi_n}{\rho A} (A_{T1}e^{j\omega_{Tn1}t} + A_{T2}e^{j\omega_{Tn2}t} + A_{T3}e^{j\omega_{Tn3}t} + A_{T4}e^{j\omega_{Tn4}t} + A_{T5}e^{j\varpi_n t} + A_{T6}e^{-j\varpi_n t}) \sin(n\pi z/\ell), \tag{5}$$

where  $A_{T1} \sim A_{T4}$  are listed in the appendix. There are four natural frequencies,  $\omega_{Tn1} \sim \omega_{Tn4}$  corresponding to two forward and two backward frequencies, respectively. However, those frequencies have no explicit form and must be determined numerically.

(c) *Rayleigh beam model:*

$$u_R(z, t) = (2/\ell) \sum_{n=1}^{\infty} \frac{d_R P\varpi_n}{a_R} (A_{R1}e^{j\omega_{Rn1}t} + A_{R2}e^{j\omega_{Rn2}t} + A_{R3}e^{j\varpi_n t} + A_{R4}e^{-j\varpi_n t}) \sin\left(\frac{n\pi z}{\ell}\right). \tag{6}$$

Here,  $A_{R1} \sim A_{R4}$  are listed in appendix,  $d_R = 1$  and the natural frequencies are

$$\omega_{Rn1,Rn2} = \frac{b_R\Omega \pm \sqrt{a_R c_R + b_R^2\Omega^2}}{a_R}, \tag{7}$$

where  $a_R = \rho A + \rho I(n\pi/\ell)^2$ ,  $b_R = \rho I(n\pi/\ell)^2$  and  $c_R = EI(n\pi/\ell)^4$ . There are two natural frequencies with explicit forms. Comparing Eq. (3) with Eqs. (6) and (4) with Eq. (7), one can notice that the shaft deflection and the natural frequencies are different between the modified-Rayleigh and the Rayleigh beam models due to different values of the coefficients denoted by  $a_R$ ,  $a_L$ ,  $d_R$  and  $d_L$ . However both natural frequencies can be expressed in close forms.

The dimensionless moving load speed, shaft deflection, rotational speed and Rayleigh beam coefficient are defined as

$$Z = z/\ell, \quad \alpha = v/v_{cr}, \quad \bar{u} = u/u_s, \quad \lambda = \Omega/\omega_{1EB}, \quad \beta = \frac{\pi r_0}{\ell}, \tag{8}$$

where  $Z$  is the non-dimensional position along the rotating shaft,  $v_{cr} = \pi/\ell \sqrt{EI/\rho A}$  is the fundamental critical speed of a pinned–pinned, non-rotating Euler–Bernoulli beam,  $\beta$  is the Rayleigh beam coefficient,  $r_0$  is the radius of gyration,  $\omega_{1EB}$  and  $u_s = P\ell^3/48 EI$  are the first natural frequency and the static deflection at midspan of a pinned–pinned Euler–Bernoulli beam. With the rotational speed  $\lambda$  ranging from 0 to 10, the first and the second forward natural frequencies of a simply supported beam with parameters,  $\kappa = 0.9$ ,  $E = 207 \text{ GPa}$ ,  $G = 77.6 \text{ GPa}$  are plotted in Fig. 2 for  $\beta = 0.15$  and Fig. 3 for  $\beta = 0.35$ , respectively. Note that the frequency with a smaller value is selected from the two forward frequencies of the Timoshenko beam model

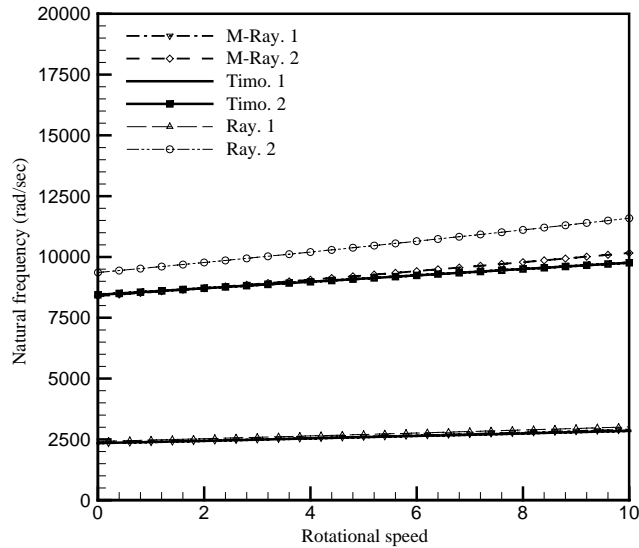


Fig. 2. Comparison of forward frequencies,  $\beta = 0.15$ .

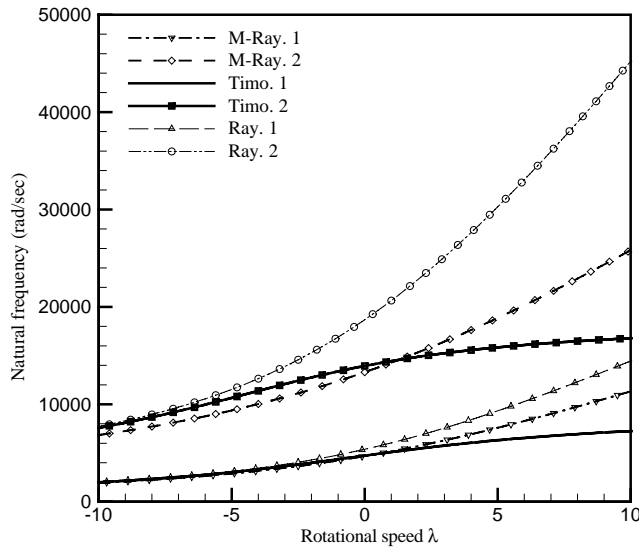


Fig. 3. Comparison of forward frequencies,  $\beta = 0.35$ .

because the response is dominated by the lower frequency while the excitation is a moving load with constant amplitude. Compared with the Rayleigh beam model, the first and second forward natural frequencies predicted by the modified-Rayleigh beam model are much closer to those calculated by the Timoshenko beam model for both  $\beta = 0.15$  and  $0.35$ .

In order to quantify the difference in the estimation of the deflection using the respective beam model, a measure of deviation of the maximum deflection is defined as

$$D_{L(or R)i} \% = \frac{|(u_i/u_s)_T - (u_i/u_s)_{L(orR)}|}{|(u_i/u_s)_T|} 100\%, \tag{9}$$

where the subscript  $i = x$  or  $y$ . The differences in the maximum values of  $u_x/u_s$  and  $u_y/u_s$  between the Timoshenko and modified-Rayleigh beam models, denoted by  $D_{Lx}$  and  $D_{Ly}$ , the Timoshenko and Rayleigh beam models,  $D_{Rx}$  and  $D_{Ry}$ , of a rotating shaft for varying  $\alpha$ ,  $\beta$ , and  $\lambda$  are listed in Tables 1–4. Based on the presented numerical data, the deflection predicted by the modified-Rayleigh beam has improved a lot, e.g., within the range,  $\alpha \leq 1.5$ ,  $\beta \leq 0.15$  and  $\lambda \leq 5$ , the deviation  $D_{Lx} \leq 0.5\%$  compared with  $D_{Rx} \leq 9.11\%$ . On the other hand, the deviation in the deflections  $u_y$  is  $D_{Ly} \leq 21\%$  compared with  $D_{Ry} \leq 28\%$  within the range  $\alpha \leq 1.5$ ,  $\beta \leq 0.15$  and  $\lambda \leq 5$ . The prediction of the deflection in  $y$  direction has not improved as much as that in  $x$  direction. However, one should

Table 1  
Comparisons of the maximum values of  $u_x/u_s$  between Timoshenko and modified-Rayleigh beam model,  $D_{Lx} \%$

$\alpha$	$\lambda=0$			$\lambda=2.5$			$\lambda=5$		
	$\beta=0.03$	$\beta=0.15$	$\beta=0.35$	$\beta=0.03$	$\beta=0.15$	$\beta=0.35$	$\beta=0.03$	$\beta=0.15$	$\beta=0.35$
0.11	0.0010	0.0781	0.553	0.0000	0.1126	2.376	0.0010	0.0703	1.580
0.30	0.0007	0.0945	1.235	0.0000	0.0413	3.697	0.0000	0.2993	3.715
0.45	0.0006	0.1739	0.517	0.0000	0.0225	1.411	0.0006	0.4881	10.707
0.50	0.0006	0.1716	0.750	0.0006	0.2320	1.420	0.0000	0.4977	9.788
0.70	0.0015	0.0256	1.282	0.0015	0.1487	2.648	0.0015	0.4447	11.902
0.90	0.0048	0.3470	2.321	0.0039	0.3022	5.082	0.0039	0.1356	18.835
1.10	0.0034	0.0960	2.900	0.0023	0.0964	10.122	0.0023	0.1481	21.888
1.30	0.0014	0.1028	3.328	0.0000	0.0206	21.026	0.0000	0.2181	30.935
1.50	0.0066	0.1455	104.0	0.0083	0.0314	94.095	0.0066	0.3025	71.605
2.10	0.0206	0.0115	126.8	0.0206	0.3098	147.57	0.0206	1.1690	479.58

Table 2  
Comparisons of the maximum values of  $u_x/u_s$  between Timoshenko and Rayleigh beam model,  $D_{Rx} \%$

$\alpha$	$\lambda=0$			$\lambda=2.5$			$\lambda=5$		
	$\beta=0.03$	$\beta=0.15$	$\beta=0.35$	$\beta=0.03$	$\beta=0.15$	$\beta=0.35$	$\beta=0.03$	$\beta=0.15$	$\beta=0.35$
0.11	0.348	9.49	34.41	0.349	9.39	28.55	0.353	8.29	32.38
0.30	0.375	8.97	33.30	0.374	9.03	35.69	0.374	9.11	19.73
0.45	0.342	7.51	25.66	0.342	7.58	33.60	0.341	7.68	43.24
0.50	0.324	7.03	25.23	0.323	7.10	32.85	0.323	7.19	44.50
0.70	0.103	4.15	30.89	0.103	4.34	31.72	0.104	4.92	43.34
0.90	0.388	9.27	32.88	0.388	8.95	36.17	0.388	8.27	43.64
1.10	0.467	7.98	35.19	0.469	8.20	39.46	0.470	8.78	48.89
1.30	0.327	7.18	38.53	0.327	7.44	43.49	0.327	8.04	53.87
1.50	0.126	8.64	43.49	0.126	8.53	49.75	0.124	8.20	59.06
2.10	0.395	7.72	569.3	0.395	7.65	637.2	0.392	7.82	1836.

Table 3

Comparisons of the maximum values of  $u_y/u_s$  between Timoshenko and modified-Rayleigh beam model,  $D_{Ly}$  %

$\alpha$	$\lambda = 1.5$			$\lambda = 2.5$			$\lambda = 5$		
	$\beta = 0.03$	$\beta = 0.15$	$\beta = 0.35$	$\beta = 0.03$	$\beta = 0.15$	$\beta = 0.35$	$\beta = 0.03$	$\beta = 0.15$	$\beta = 0.35$
0.11	0.764	1.985	198.7	0.518	3.782	211.3	0.249	1.677	16.30
0.30	0.303	5.944	33.17	0.283	6.197	24.85	0.247	7.262	7.052
0.45	0.307	9.432	33.17	0.309	8.535	34.10	0.318	6.608	32.87
0.50	0.385	8.379	36.78	0.385	7.523	36.66	0.379	5.740	35.74
0.70	0.487	5.409	54.40	0.486	5.244	52.90	0.482	4.848	47.78
0.90	0.449	16.87	87.70	0.449	16.09	82.82	0.450	13.07	66.65
1.10	0.539	10.31	143.8	0.539	10.50	134.4	0.543	11.14	97.51
1.30	0.973	16.10	236.1	0.970	16.05	221.1	0.956	16.02	159.1
1.50	0.937	20.56	285.1	0.932	20.52	274.8	0.915	20.42	227.9
2.10	2.131	45.20	14.42	2.122	45.12	11.34	2.085	44.67	5.473

Table 4

Comparisons of the maximum values of  $u_y/u_s$  between Timoshenko and Rayleigh beam model,  $D_{Ry}$  %

$\alpha$	$\lambda = 1.5$			$\lambda = 2.5$			$\lambda = 5$		
	$\beta = 0.03$	$\beta = 0.15$	$\beta = 0.35$	$\beta = 0.03$	$\beta = 0.15$	$\beta = 0.35$	$\beta = 0.03$	$\beta = 0.15$	$\beta = 0.35$
0.11	2.133	2.685	163.7	2.104	1.971	182.2	1.783	9.274	22.37
0.30	0.678	24.40	204.3	0.687	20.55	11.78	0.728	7.296	26.96
0.45	0.283	0.001	24.42	0.282	0.815	14.58	0.270	1.957	6.851
0.50	0.674	0.984	26.85	0.660	1.021	16.93	0.612	0.573	2.570
0.70	1.613	27.80	1.260	1.601	26.67	6.139	1.532	23.37	8.468
0.90	0.329	7.555	11.26	0.328	7.619	8.854	0.345	7.914	10.02
1.10	2.698	7.366	23.68	2.689	6.629	21.42	2.656	4.716	14.22
1.30	0.972	17.33	47.71	0.972	16.27	44.64	0.978	12.84	36.51
1.50	2.821	0.079	125.3	2.814	0.259	121.2	2.794	1.983	109.0
2.10	2.049	11.65	343.0	2.071	12.86	333.7	2.160	15.76	310.9

note that the deflection  $u_y$  is only 9% of  $u_x$  within the range,  $\alpha \leq 1.5$ ,  $\beta \leq 0.15$  and  $\lambda \leq 5$ . In other words, the deflection of the shaft is dominated by  $u_x$ . Nevertheless,  $u_y$  will increase mainly due to the gyroscopic effect for higher rotational speeds  $\lambda$ . One can predict that the influences from the associated coupling effects induced from the shear deformation increase as the rotational speed and the Rayleigh beam coefficient increase. In fact,  $\alpha \leq 1.5$ ,  $\beta \leq 0.15$  and  $\lambda \leq 5$  in which the modified-Rayleigh beam has a close approximation to the Timoshenko beam, covers most of the rotating shaft operating conditions in engineering application.

#### 4. Comparisons of the critical speed

A critical speed is said to exist when the frequency of the rotation of a shaft equals one of the natural frequencies of the shaft. A rapid transition of the rotating shaft through a critical speed is

expected to limit the whirl amplitudes. Therefore, a correct prediction of the critical speed is crucial in determining the vibration characteristics of a shaft. For the purpose of consistency, the dimensionless parameters introduced here are the same as those in [6]

$$U = \frac{u}{\ell}, \quad c = \sqrt{\frac{\rho A \ell^4}{EI}} \Omega, \quad \tau = \Omega t, \quad \sigma = \frac{1}{\delta} \left( \frac{\pi}{\beta} \right)^2, \tag{10}$$

where  $\delta = 2(1 + \mu)/\kappa$  and  $\mu$  is the Poisson ratio. Let the moving force be absent and the dimensionless equations of motion for the respective beam models are given as follows:

(a) *Timoshenko beam model:*

$$\frac{\partial^4 U}{\partial Z^4} + 2jr^2 c^2 \frac{\partial^3 U}{\partial Z^2 \partial \tau} - r^2 c^2 (\delta + 1) \frac{\partial^4 U}{\partial Z^2 \partial \tau^2} + c^2 \frac{\partial^2 U}{\partial \tau^2} - 2jr^4 c^4 \delta \frac{\partial^3 U}{\partial \tau^3} + r^4 c^4 \delta \frac{\partial^4 U}{\partial \tau^4} = 0. \tag{11}$$

(b) *Modified-Rayleigh beam model:*

$$\frac{\partial^4 U}{\partial Z^4} + 2jr^2 c^2 \frac{\partial^3 U}{\partial Z^2 \partial \tau} - r^2 c^2 (\delta + 1) \frac{\partial^4 U}{\partial Z^2 \partial \tau^2} + c^2 \frac{\partial^2 U}{\partial \tau^2} = 0. \tag{12}$$

(c) *Rayleigh beam model:*

$$\frac{\partial^4 U}{\partial Z^4} + 2jr^2 c^2 \frac{\partial^3 U}{\partial Z^2 \partial \tau} - r^2 c^2 \frac{\partial^4 U}{\partial Z^2 \partial \tau^2} + c^2 \frac{\partial^2 U}{\partial \tau^2} = 0. \tag{13}$$

After some manipulations, the critical speed  $c_n$  corresponding to the  $n$ th flexural mode of the respective beam model is:

(a) *Timoshenko beam model:*

$$c_n = \pm \frac{\pi^2}{\sqrt{2\delta\beta^2}} \sqrt{-1 - (\delta - 1)n^2\beta^2 \pm \sqrt{4n^4\delta\beta^4 + [1 + (\delta - 1)n^2\beta^2]^2}}. \tag{14}$$

(b) *Modified-Rayleigh beam model:*

$$c_n = \pm \frac{n^2\pi^2}{\sqrt{1 + (\delta - 1)n^2\beta^2}}. \tag{15}$$

(c) *Rayleigh beam model:*

$$c_n = \pm \frac{n^2\pi^2}{\sqrt{1 - n^2\beta^2}}. \tag{16}$$

Comparing Eqs. (15) and (16), the term,  $n^2$  in Rayleigh beam model is simply replaced by  $(\delta - 1)n^2$  in the modified-Rayleigh beam model. For  $\mu = \frac{1}{3}$ ,  $\delta$  is always greater than 1 for a steel shaft of a circular cross-section. Therefore, Eq. (16) indicates that there exists an infinite number of possible critical speeds as the Timoshenko beam model due to the inclusion of the shear deformation. However, the Rayleigh beam model predicts only a finite number of critical speeds, which is not true in reality.

The critical speed for a rotating shaft within the Rayleigh beam coefficient  $\beta$  ranging from 0.01 to 2 is plotted in Fig. 4 for the first three forward and three backward frequencies. It is shown that the critical speeds derived from the modified-Rayleigh beam model and those from the



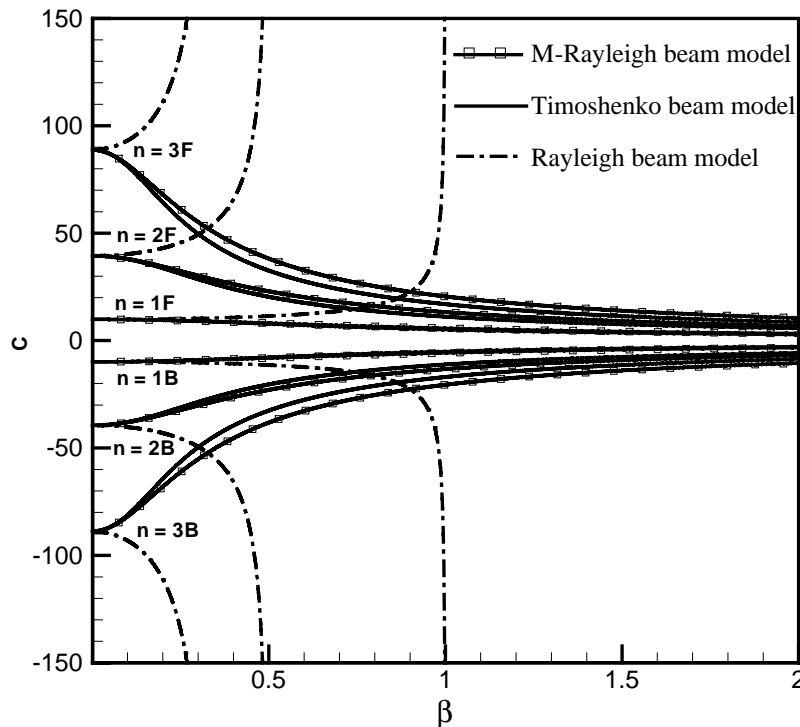


Fig. 4. Comparison of the natural frequency predicted by the respective beam models.

Timoshenko beam model decrease as the  $\beta$  increases. The trends of critical speeds corresponding to different flexural modes are similar and close to each other with respect to the varying  $\beta$ . On the contrary, the critical speeds predicted from the Rayleigh beam model increases as the  $\beta$  increases. Moreover, the critical speeds corresponding to the  $n$ th flexural mode increase beyond bound when  $\beta = 1/n$ . Eventually the number of critical speeds predicted by the Rayleigh beam model is limited and is acceptable only for a small value of  $\beta$ , i.e.,  $\beta < 0.1$ .

## 5. Conclusion

A modified-Rayleigh beam is proposed to improve the prediction accuracy of the critical speed, the natural frequency and the shaft deformation of the Rayleigh beam model subjected to a moving load. This beam model takes into account the shear deformation effect but it neglects the associate coupling effects induced by the shear deformation; such as the coupling between transverse shear and the gyroscopic effects and the coupling between transverse shear and the rotary inertia. The main advantage is that the natural frequencies of a high-speed spinning, short and stubby shaft can be determined analytically and the estimations agree well with those calculated numerically using the Timoshenko beam model. Results have also shown that good agreement in maximum deflection can be achieved quantitatively between the Timoshenko beam

and the modified-Rayleigh beam for a high-speed rotational shaft, i.e.,  $D_L \leq 0.5\%$  for  $\alpha \leq 1.5$ ,  $\beta \leq 0.15$ ,  $\lambda \leq 5$ .

## Appendix A

The coefficients  $A_{T1} \sim A_{T4}$  in Eq. (5) are listed as follows:

$$A_{T1} = j(\omega_{Tn1}^2 - 2\Omega\omega_{Tn1} - b^2)/[(\omega_{Tn1} - \omega_{Tn2})(\omega_{Tn1} - \omega_{Tn3})(\omega_{Tn1} - \omega_{Tn4})(\omega_{Tn1}^2 - \varpi_n^2)],$$

$$A_{T2} = j(\omega_{Tn2}^2 - 2\Omega\omega_{Tn2} - b^2)/[(\omega_{Tn2} - \omega_{Tn1})(\omega_{Tn2} - \omega_{Tn3})(\omega_{Tn2} - \omega_{Tn4})(\omega_{Tn2}^2 - \varpi_n^2)],$$

$$A_{T3} = j(\omega_{Tn3}^2 - 2\Omega\omega_{Tn3} - b^2)/[(\omega_{Tn3} - \omega_{Tn1})(\omega_{Tn3} - \omega_{Tn2})(\omega_{Tn3} - \omega_{Tn4})(\omega_{Tn3}^2 - \varpi_n^2)],$$

$$A_{T4} = j(\omega_{Tn4}^2 - 2\Omega\omega_{Tn4} - b^2)/[(\omega_{Tn4} - \omega_{Tn1})(\omega_{Tn4} - \omega_{Tn2})(\omega_{Tn4} - \omega_{Tn3})(\omega_{Tn4}^2 - \varpi_n^2)],$$

$$A_{T5} = j(\varpi_n^2 - 2\Omega\varpi_n - b^2)/[2\varpi_n(\varpi_n - \omega_{Tn1})(\varpi_n - \omega_{Tn2})(\varpi_n - \omega_{Tn3})(\varpi_n - \omega_{Tn4})],$$

$$A_{T6} = -j(\varpi_n^2 + 2\Omega\varpi_n - b^2)/[2\varpi_n(\varpi_n + \omega_{Tn1})(\varpi_n + \omega_{Tn2})(\varpi_n + \omega_{Tn3})(\varpi_n + \omega_{Tn4})].$$

The coefficients  $A_{L1} \sim A_{L4}$  in Eq. (6) are listed as follows:

$$A_{L1} = j/[(\omega_{Ln1} - \omega_{Ln2})(\omega_{Ln1}^2 - \varpi_n^2)],$$

$$A_{L2} = j/[(\omega_{Ln2} - \omega_{Ln1})(\omega_{Ln2}^2 - \varpi_n^2)],$$

$$A_{L3} = j/[2\varpi_n(\varpi_n - \omega_{Ln1})(\varpi_n - \omega_{Ln2})],$$

$$A_{L4} = -j/[2\varpi_n(\varpi_n + \omega_{Ln1})(\varpi_n + \omega_{Ln2})].$$

The coefficients  $A_{R1} \sim A_{R4}$  in Eq. (3) are listed as follows:

$$A_{R1} = j/[(\omega_{Rn1} - \omega_{Rn2})(\omega_{Rn1}^2 - \varpi_n^2)],$$

$$A_{R2} = j/[(\omega_{Rn2} - \omega_{Rn1})(\omega_{Rn2}^2 - \varpi_n^2)],$$

$$A_{R3} = j/[2\varpi_n(\varpi_n - \omega_{Rn1})(\varpi_n - \omega_{Rn2})],$$

$$A_{R4} = -j/[2\varpi_n(\varpi_n + \omega_{Rn1})(\varpi_n + \omega_{Rn2})].$$

## Appendix B. Nomenclature

$A$	shaft cross-sectional area
$c_n$	critical speed corresponding to the $n$ th flexural mode
$D_{R,L}$	measure of deviation of the maximum deflection
$E$	elastic modulus
$P$	moving force amplitude
$G$	complex shear modulus
$h$	height of the beam

$I$	shaft cross-sectional second moment of inertia
$j$	$\sqrt{-1}$
$\kappa$	cross-sectional shape factor
$\ell$	shaft length
$u(z, t)$	complex transverse displacement of the shaft
$u_s$	static deflection at midspan of an unrotating Euler–Bernoulli beam = $P\ell^3/48 EI$
$u_x$	Cartesian component of the deflection along the $x$ direction
$u_y$	Cartesian component of the deflection along the $y$ direction
$v$	moving force speed
$v_{cr}$	fundamental critical speed of a pinned–pinned, unrotating Euler–Bernoulli beam
$Z$	non-dimensional position along the rotating shaft
$\beta$	Rayleigh beam coefficient
$r_0$	radius of gyration
$\alpha$	non-dimensional moving load speed
$\bar{u}$	non-dimensional transverse displacement of the shaft
$\lambda$	non-dimensional rotational speed
$\mu$	the Poisson ratio
$\rho$	beam density
$\Omega$	shaft rotating speed
$\omega_{1EB}$	first natural frequency of an Euler–Bernoulli beam with pinned supports at both ends
$\omega_{Ln,1,2}$	forward and backward frequencies of the modified-Rayleigh shaft
$\omega_{Tn,1,2,3,4}$	forward and backward frequencies of the modified Timoshenko shaft
$\omega_n$	natural frequency corresponding to the $n$ th flexural mode of the shaft
$\omega_{Rn,1,2}$	forward and backward frequencies of the Rayleigh shaft
$\varpi_n$	frequency caused by the moving load

## References

- [1] A. Tondl, Some Problems of Rotor Dynamics, Chapman & Hall, London, England, 1965.
- [2] J.S. Rao, Rotor Dynamics, Wiley Eastern, India, 1983.
- [3] A.D. Dimarogonas, S.A. Paipetis, Analytical Methods in Rotor Dynamics, Applied Science, England, 1983.
- [4] R. Katz, C.W. Lee, A.G. Ulsoy, R.A. Scott, Modal analysis of a distributed parameter rotating shaft, Journal of Sound and Vibration 122 (1) (1988) 119–130.
- [5] F.F. Ehrich, Handbook of Rotordynamics, McGraw-Hill, New York, 1992.
- [6] C.W. Lee, Vibration Analysis of Rotors, Kluwer Academic, Dordrecht, Netherlands, 1993.
- [7] R. Katz, C.W. Lee, A.G. Ulsoy, R.A. Scott, The dynamic response of a rotating shaft subject to a moving load, Journal of Sound and Vibration 122 (1) (1988) 131–148.
- [8] R.P.S. Han, J.W.Z. Zu, Modal analysis of rotating shafts: a body-fixed axis formulation approach, Journal of Sound and Vibration 156 (1) (1992) 1–16.
- [9] S.H. Choi, C. Pierre, A.G. Ulsoy, Consistent modeling of rotating Timoshenko shafts subject to axial loads, American Society Mechanical Engineers, Journal of Vibration and Acoustics 114 (1992) 249–259.
- [10] H.P. Lee, Dynamic response of a rotating Timoshenko shaft subject to axial forces and moving loads, Journal of Sound and Vibration 181 (1) (1995) 169–177.